Multiple Substrate Growth Kinetics of *Leptothrix discophora* SP-6

Nurdan Yurt,[†,‡] John Sears,[†,‡] and Zbigniew Lewandowski*[,†,§]

Center for Biofilm Engineering, Chemical Engineering Department, and Civil Engineering Department, Montana State University, EPS 366, Bozeman, Montana 59717

The growth parameters of *Leptothrix discophora* SP-6 were quantified on the basis of the steady-state concentrations and utilization rates of pyruvate, dissolved oxygen, and concentration of microorganisms in a chemostat operated at 25 °C, pH 7.2, and an agitation rate of 350 rpm. The results showed that the microbial growth was limited by both pyruvate and dissolved oxygen. A combined growth kinetics model using Monod growth kinetics for pyruvate and Tessier growth kinetics for oxygen showed the best correlation with the experimental data when analyzed using an interactive multiple substrate model. The growth kinetics parameters and the respective confidence limits, estimated using the Monte Carlo simulation, were $\mu_{max} = 0.576 \pm 0.021$ h^{-1}, $K_{sMp} = 38.81 \pm 4.24$ mg L^{-1}, $K_{sTo} = 0.39 \pm 0.04$ mg L^{-1}, $Y_{X/p} = 0.150$ (mg microorganism mg^{-1} pyruvate), $Y_{X/o} = 1.24$ (mg microorganism mg^{-1} oxygen), the maintenance factors for pyruvate and oxygen were $m_p = 0.129$ (mg pyruvate consumed mg^{-1} microorganism h^{-1}) and $m_o = 0.076$ (mg oxygen consumed mg^{-1} microorganism h^{-1}), respectively.

Introduction

Leptothrix discophora SP-6 is a member of the *Sphaerotilus Leptothrix* group, manganese- and iron-oxidizing sheathed bacteria that thrive in iron- and manganese-rich environments such as iron seeps, swamps, and springs (Emerson and Ghiorse, 1992). Although *Leptothrix discophora* are not pathogens, they are considered a nuisance in water distribution systems because they oxidize iron and manganese, cause color problems, and in extreme cases clog water distribution conduits. In our laboratory, we have been quantifying the metabolic activity of biofilms of manganese-oxidizing bacteria and their effect on microbially influenced corrosion (MIC), specifically on pitting corrosion of stainless steels (Dickinson and Lewandowski, 1996; Dickinson et al., 1996; Olesen et al., 2000a; Olesen et al., 2000b) using *Leptothrix discophora* SP-6, which forms biofilms and oxidizes Mn^{2+} to manganese oxides, as a model microorganism. To construct the mathematical models of MIC caused by manganese oxidizing bacteria we attempt to evaluate two factors: (1) the growth kinetics of the microorganisms involved, and (2) the rate of manganese oxide deposition in biofilms deposited on metal surfaces. This paper deals with the first factor, the growth kinetics of the model manganese-oxidizing bacteria, *Leptothrix discophora* SP-6.

The goal of this study was to represent the growth rate of *Leptothrix discophora* SP-6 by a suitable mathematical model and to calculate biokinetic parameters associated with this model. To simplify calculating the growth parameters from the chemostat data, researchers often use a single substrate in the growth model. However, it is well-known that the microbial growth rate often depends on more than one substrate (Machado et al., 1989; Beyenal and Tanyolac, 1997; Neeleman et al., 2001). To take into account such a possibility, we operated a chemostat, quantified the steady-state growth parameters based on the mass balances for pyruvate, dissolved oxygen, and microorganisms and their respective concentrations, and used MATLAB programming to estimate biokinetic parameters by testing whether single or double substrate growth models predict the specific growth rate better.

Materials and Methods

Microorganisms. Frozen stock culture of *Leptothrix discophora* SP-6 (ATCC no. 51168) was obtained from the American Type Culture Collection (ATCC), and the stock cultures that we used were prepared by following the procedures described in the ATCC catalog. As soon as a frozen vial was received, it was placed in a deep freezer (−70 °C). For propagation, the vial was thawed rapidly by agitating in a 37 °C water bath. Then, the microorganisms were transferred aseptically into a flask containing 10 mL of the sterile ATCC no. 1917 broth (Table 1). The flask was incubated at 20 °C for 2−4 days, and after the microbial growth had been detected, the content of the flask was transferred to 100 mL of a fresh broth. The cells were harvested in the early stationary phase of growth (after 30−40 h) and pelleted by centrifugation using sterile centrifuge tubes (50 mL each). The supernatant was discarded, and the pellets were resuspended in 100 mL of 5% sterile broth + 20% sterile glycerol. Finally, 1-mL aliquots of the suspension were dispensed into small sterile vials and stored at −70 °C. When needed, they were removed, thawed in a 37 °C water bath, and inoculated into fresh ATCC no. 1917 broth medium.

The inoculum was prepared as follows: 1 mL of frozen stock culture of *Leptothrix discophora* SP-6 (ATCC no. 51168) was poured into an Erlenmeyer flask containing 100 mL of sterile growth media (A and B) prepared as described in Table 1. The microorganisms were grown in the Erlenmeyer flasks, without stirring, for 30−40 h

* To whom correspondence should be addressed. Tel: 406-994-5915. Fax: 406-994-6098. Email: ZL@erc.montana.edu.
[†] Center for Biofilm Engineering.
[‡] Chemical Engineering Department.
[§] Civil Engineering Department.

10.1021/bp0255098 CCC: $22.00
Published on Web 07/25/2002

Table 1. ATCC Culture 1917 MSVP for *Leptothrix discophora* SP-6 (American Type Culture Collection Catalog, 1992)

medium A[a]	
$(NH_4)_2SO_4$	0.24 g
$MgSO_4 \cdot 7H_2O$	0.06 g
$CaCl_2 \cdot 2H_2O$	0.06 g
KH_2PO_4	0.02 g
$Na_2HPO_4 \cdot 7H_2O$	0.06 g
HEPES buffer	2.383 g
distilled water to	984 mL
medium B	
20% sodium pyruvate	5 mL
$FeSO_4$ 10 mM	1 mM
vitamin solution	1 mL
vitamin solution	
biotin	20.0 mg
folic acid	20.0 mg
thiamine HCl	50.0 mg
D-(+)-calcium pantothenate	50.0 mg
vitamin B12	1.0 mg
riboflavin	50.0 mg
nicotinic acid	50.0 mg
pyridoxine HCl	100.0 mg
p-aminobenzoic acid	50.0 mg
distilled water to	1.0 L

[a] The pH of medium A was adjusted to 7.2 with NaOH or H_2SO_4. Medium A was then autoclaved at 121 °C for 15 min (for 1 L volume of the solution). After it cooled to approximately 50 °C, filter-sterilized (0.2 μm sterile syringe filter, Corning, 431219) medium B solutions were added into the autoclaved medium A aseptically. HEPES is *N*-2-hydroxyethylpiperazine-*N*′-2-ethanesulfonic acid.

at room temperature, and the chemostat was inoculated with 200 mL of this culture.

Chemostat. The microorganisms were grown in a New Brunswick (BioFlo 2000) chemostat with a 2-L working volume and equipped with pH, agitation, and temperature controllers. The sensitivities of the control units were 0.1 unit, 0.1 °C, ±1 rpm for pH, for temperature, and for agitation rate, respectively. Prior to use, the chemostat and the medium A (Table 1) were autoclaved for 30 min at 121 °C. Then the medium B (Table 1) was aseptically syringed into medium A using 0.2-μm filters (Corning, 431219). The pH was controlled by adding solutions of 0.2 N NaOH and 0.2 N H_2SO_4, when needed. The solution in the chemostat was stirred by a double blade type impeller at 350 rpm, and the stirring rate was optimized (results not shown) using the specific oxygen uptake rate as the criterion. We compared the specific oxygen uptake rates measured at a fixed dilution rate (0.1 h^{-1}) and at different agitation rates (150, 250, 350, 450, and 550 rpm). We found that the optimum agitation rate was 350 rpm. At low agitation rates, *Leptothrix discophora* SP-6 aggregated, and at higher agitation rates it was mechanically damaged. The steady-state dissolved oxygen concentrations measured at different dilution rates were between 0.1 and 7.8 mg L^{-1}. The dissolved oxygen concentration was controlled by sparging the filtered air, or filtered mixtures of the air + pure oxygen or air + nitrogen in various proportions, depending on the needs, at flow rates between 1 and 5 L h^{-1}.

The chemostat was inoculated with the microorganisms using 10% (volume of the inoculum/total working volume of the chemostat) inoculum harvested during the exponential growth phase from a batch culture flask. Initially, the chemostat was run in a batch mode and then in a continuous flow mode after the culture had reached the exponential growth phase (usually after 30−40 h). To reach the steady state, the chemostat was operated for six or seven retention times and the existence of the steady state was verified by checking that the absolute differences in effluent substrate concentrations differed by less than 3 % in consecutive measurements of corresponding retention times. The following parameters were measured at steady state: dissolved oxygen and microorganism concentrations, influent and effluent pyruvate concentrations, oxygen consumption rate, dilution rate, pH, and temperature. New steady states were established by gradually increasing the dilution rates to the desired levels, to the washout point. The microbial culture was periodically examined for contamination by plating on agar plates. We continuously monitored biofilm formation on the reactor walls and, when it was necessary, the reactor was shut off to clean the biofilm and then restarted.

Analytical Methods. Pyruvate concentration was determined using a Dionex (Sunnyvale, CA) ion chromotograph (model DX 300) equipped with an autosampler (25-μL sample loop), an IonPAC AS10 analytical column (Dionex P/N 43118), an ion suppresser, a conductivity detector, and Peaknet software. The eluant was 3.5 mM potassium tetraborate with a flow rate of 1.0 mL min^{-1}. The retention time for pyruvate was 5.5 min. Before the next injection, the column was washed for 3 min with 100 mM potassium tetraborate and returned to initial conditions.

The microorganism concentration was determined using the Standard Volatile Solids Method (Eaton et al., 1995).

Dissolved oxygen concentration was monitored by the Ingold dissolved oxygen probe, and pH was monitored the Mettler Toledo pH electrodes, all integrated with the chemostat (New Brunswick, BioFlo 2000).

The oxygen uptake rate was estimated using a procedure described by Bandyopdhyay et al. (1967). Before each measurement, the aeration was stopped and the gas space in the chemostat was flushed with nitrogen to remove oxygen and prevent reaeration. Immediately after, the dissolved oxygen concentration in the reactor was determined and recorded against time. The rate of oxygen consumption, dS_O/dt, determined as the slope of the plot of oxygen concentration versus time at the linear region, was equivalent to the oxygen uptake rate. The specific oxygen uptake rate (SOUR) was determined by dividing the oxygen uptake rate by the biomass concentration ($dS_O/dt/X$). We also tested the effect of oxygen transfer from the liquid to the gas phase on SOUR by replacing air with nitrogen in the headspace of the chemostat and measuring dS_O/dt at two gas flow rates, 0 and 10 L min^{-1}, and found that this effect was negligible.

Selecting the Growth Model and Estimating the Kinetic Constants. According to Bailey and Ollis (1986), when microbial growth is limited by more than one substrate, three forms of multiple substrate growth kinetics can be considered:

(1) an interactive or multiplicative form:

$$\mu/\mu_{max} = [\mu(S_1)]\,[\mu(S_2)]\,\ldots\,[\mu(S_i)] \qquad (1)$$

(2) an additive form:

$$\mu/\mu_{max} = [\mu(S_1) + \mu(S_2) + \ldots + \mu(S_i)]/i \qquad (2)$$

(3) a noninteractive form:

$$\mu/\mu_{max} = \mu(S_1) \text{ or } \mu(S_2) \text{ or } \ldots \text{ or } \mu(S_i) \qquad (3)$$

Table 2. Combined and Single Growth Models Were Used to Find the Best Model, and the Corresponding Biokinetic Coefficients

model no.	multiple model eq no.	single model eq no. for pyruvate	single model eq no. for oxygen
1	3		
2	3		4
3	3		5
4	3		6
5	3		7
6	3	4	
7	1	4	4
8	1	4	5
9	1	4	6
10	1	4	7
11	3	5	
12	1	5	4
13	1	5	5
14	1	5	6
15	1	5	7
16	3	6	
17	1	6	4
18	1	6	5
19	1	6	6
20	1	6	7
21	3	7	
22	1	7	4
23	1	7	5
24	1	7	6
25	1	7	7

On the basis of preliminary results, we selected pyruvate and oxygen as the substrates limiting microbial growth in our chemostat (see Results and Discussion). The additive form (eq 2) was not applicable because it implied that the microorganisms would grow on either of the limiting substrates, pyruvate or oxygen, which was not the case. We demonstrated that microbial growth in the chemostat was negligible in the absence of either oxygen or pyruvate.

Many mathematical models describe microbial growth rate as a function of single substrate concentration (see Bailey and Ollis, 1986 for details). To develop multiple substrate growth kinetics, these individual microbial growth models are combined in a manner described by eqs 1−3 (Shuler and Kargi, 1992). In this study, we considered the following often used empirical expressions describing single substrate growth models of suspended microorganisms (Panikov, 1995):

$$\text{Monod: } \mu = \mu_{\max}\frac{S_i}{K_{\text{sM}i} + S_i} \quad \text{(Monod, 1949)} \tag{4}$$

$$\text{Tessier: } \mu = \mu_{\max}(1 - e^{-S_i/K_s T}) \quad \text{(Tessier, 1942)} \tag{5}$$

$$\text{Moser: } \mu = \mu_{\max}(1 + K_{\text{sMZ}i}S_i^{-\lambda_i})^{-1} \quad \text{(Moser, 1958)} \tag{6}$$

$$\text{Contois: } \mu = \mu_{\max}\frac{S_i}{B_i X + S_i} \quad \text{(Contois, 1959)} \tag{7}$$

For each steady state, the specific growth rate, μ, was calculated as equal to dilution rate:

$$\mu = D = Q/V \tag{8}$$

This expression, where the dilution rate and the growth rate are numerically equal, is a cornerstone of the chemostat theory. However, the dilution rate, D, in this expression is an independent variable, set by the operator, while the growth rate, μ, is a dependent variable and is affected by many factors including the substrate concentration (Panikov, 1995). This distinction may pass unnoticed when using single substrate growth kinetics because for a single substrate concentration there is only one growth rate. However, this distinction becomes important where using multiple substrate growth kinetics when the growth rate depends on more than one variable. As a consequence, when using multiple substrate growth kinetics it is possible to reach multiple steady states by manipulating one substrate concentration and keeping the other substrate(s) concentration constant (as demonstrated in Table 3).

Table 3. Data Collected at Various Steady States[a]

D (h^{-1})	X (mg L^{-1})	S_P (mg L^{-1})	S_O (mg L^{-1})	SOUR[b]
0.029	87	2	5.7	0.0935
0.052	113	3.6	5.6	0.11
0.071	131	5.2	3.8	0.137
0.081	110	26.9	0.2	0.16
0.129	111	12.8	1.3	0.174
0.163	97	40.7	0.4	0.22
0.24	143	28.9	2.2	0.378
0.48	106	225	6.8	0.425
0.118	134	10.4	2.1	0.156
0.1	104	7.7	3.3	0.151
0.08	175	10.2	0.9	0.152
0.1	109	470	0.1	0.162
0.1	125	8.1	5.1	0.163
0.1	175	10.4	6	0.151
0.047	114	3.4	7.6	0.124
0.055	121	4.5	7.7	0.112
0.03	98	1.9	7.8	0.105
0.11	119	8.1	7.7	0.139
0.188	132	17.5	5.5	0.21
0.5	99	325	6.8	na
0.3	103	34.1	1.6	0.27
0.35	121	74	0.9	0.31
0.43	113	234	0.65	0.435

[a] The chemostat was operated at temperature = 25 °C, pH = 7.2, agitation rate = 350 rpm, S_{fP} = 1000 mg L^{-1}, S_{fn} = 65 mg NH_4^+ L^{-1}. [b] mg oxygen mg^{-1} microorganism h^{-1}.

Maintenance and Yield Factors. The maintenance factor, m_i, and the yield factor, $Y_{X/i}$, were calculated from mass balances on the respective substrates (pyruvate or oxygen) by rearranging the following equation:

$$D(S_{fi} - S_{ei}) = \frac{\mu_i X}{Y_{X/i}} + m_i X \tag{9a}$$

$$\frac{(S_{fp} - S_p)}{X} = \frac{m_p}{D} + \frac{1}{Y_{X/p}} \tag{9b}$$

$$\frac{\text{SOUR}}{D} = \frac{m_o}{D} + \frac{1}{Y_{X/o}} \tag{9c}$$

Equation 9b is derived from eq 9a and allows the plotting of $(S_{fp} - S_p)/X$ versus $1/D$; the slope of this plot gives m_p and the intercept gives $1/Y_{X/p}$. Equation 9c is also derived from eq 9a and it allows the plotting of SOUR/D versus $1/D$; the slope of this plot gives m_o and the intercept gives $1/Y_{X/o}$.

Nonlinear Regression To Calculate Biokinetic Parameters. We combined all possible biokinetic expressions in pairs, eqs 1 and 3 (25 combinations, see Table 2), and used the direct search method (Lagarias et al., 1998), which requires minimizing a predefined objective function to estimate the biokinetic parameters from experimental data. As the objective function, we defined the sum of squares of differences (SSD) between

the experimentally measured specific growth rates and the specific growth rates calculated by the mathematical model

$$\mathrm{SSD} = \sum_{i=1}^{N} (\mu_{\mathrm{exptl}} - \mu_{\mathrm{model}})^2 \qquad (10)$$

Specific growth rates used in the models (μ_{model}) were calculated from different combinations of eqs 4−7 and eqs 1 and 3, as shown in Table 2. SSD values calculated for each combined model are given in Table 4.

The direct search method we used (Lagarias et al., 1998) was available with the MATLAB software; we also used the MATLAB programming to calculate the biokinetic parameters. The MATLAB program we developed to select the best model and to estimate the biokinetic coefficients is given in Appendix A. As a general rule, the following restrictions were applied in the search: (1) models that produced nonrealistic biokinetic coefficients (values that were negative, extremely high, or significantly out of range of biokinetic constants reported in the literature) were rejected, and (2) if the model estimates were not stable (i.e., it produced different biokinetic parameters for different but very close initial estimates), the model was rejected as ill-conditioned. To test if the model solution depended on the initial estimates, we ran the program at least 20 times using randomly generated initial estimates and found that the solutions did not depend on initial estimates. All results of the chemostat experiments, collected in Table 3, were subjected to this procedure.

Selecting the Best Model and Running Sensitivity Analysis. The best multiple substrate growth model was selected from among the different combinations of eqs 4−7 (Table 2). Since several models yielded very close SSD values, we used the Monte Carlo simulation to determine confidence limits for the growth parameters and then selected the model that provided the narrowest confidence limits and lowest SSD. Looking for the best kinetic equation, we tested the effects of oxygen and pyruvate on the growth rate. However, there are other substances that may affect the growth rate, ammonia or micronutrients, for example, because metabolic reactions can be impeded by the deficiency of various substances. We tested the effect of ammonia on the growth rate of *Leptothtrix discophora* and made sure that its concentration in the chemostat was above the level that could limit the microbial growth. We could use ammonia as another substance to control the microbial growth and develop more complicated kinetic expressions. In principle, the number of substrates in the multiple-substrate growth kinetics does not have to be limited to two. Kinetic expressions can include any number of substances that the researcher believes are relevant; we used oxygen because *Leptothtrix discophora* is an aerobic organism and pyruvate because other sources indicated that this substance is important for growing these microorganisms (Emerson and Ghiorse, 1992; Zhang et al., 2002). This is also shown in our groups' previously published studies (Dickinson and Lewandowski, 1996; Olesen et al., 2000a,b).

To estimate the effect of measurement errors on the calculated growth parameters, random data sets (similar to those in Table 3) were generated using boot strapping Monte Carlo (Press et al., 1992). The data were generated by randomly changing the measured pyruvate concentration within the limits of ±5%, dissolved oxygen concentration within ±1%, and the measured microorganism concentration within ±10%. The limits used in each case are reasonable estimates of the experimental errors in measuring the pyruvate, dissolved oxygen, and microorganism concentrations. MATLAB's random function was also used to calculate the randomized errors from the actual data set (Table 3). To find the confidence limits for the biokinetic parameters, 1000 different randomly generated hypothetical data sets, each one within the estimated experimental errors, were used. Increasing the number of simulations above 1000 did not significantly change (up to four decimal figures) the calculated average parameters or the standard deviation values.

Results and Discussion

The experimental data in Table 3 were used to estimate growth parameters of *Leptothrix discophora* SP-6. It was also verified experimentally that the growth of *Leptothrix discophora* SP-6 in the absence of either oxygen or pyruvate was negligible (results not shown), a fact which was the basis for rejecting eq 2 as a possible growth model. It was also verified that changing NH_4^+ concentration in the feed from 5 to 150 mg/L did not affect the effluent concentrations of pyruvate, oxygen, or microorganisms (results not shown). The results in Table 3 show that both pyruvate *and* oxygen concentrations influenced the growth kinetics of *Leptothrix discophora* SP-6. Therefore, the growth of *Leptothrix discophora* SP-6 should be represented by a kinetic model taking into account double substrate limitation: pyruvate *and* oxygen. The data in Table 3 show that for the same dilution rate, 0.1 h^{-1}, the steady-state microorganism and pyruvate concentrations depended on oxygen concentration in the chemostat.

Modeling Growth Kinetics. Table 4 shows the calculated biokinetic parameters and SSD (in descending order) for the possible microbial growth models using both interactive and noninteractive combinations of eqs 4−7. Model 8 has the minimum SSD, but models 13 and 23 give low SSD values as well. To select the best growth model, the Monte Carlo simulation was used to determine the confidence limits of the calculated parameters (Table 5). Table 5 shows biokinetic parameters for these three models (8, 13, and 23), the SSD for the models, the average SSD, and the standard deviations for the Monte Carlo simulations. The average SSD for model 23 (0.132) is higher than the SSD calculated from the experimental data (0.0058), indicating that model 23 was sensitive to experimental errors; therefore this model was rejected. Models 8 and 13 showed average SSD values smaller than those of model 23 and were thereby considered better predictors of the experimental data. Because the average SSD for model 8 (0.0183) and the standard deviation for the Monte Carlo simulation (0.0069) were smaller than those for model 13, we selected model 8, Monod growth kinetics for pyruvate and Tessier growth kinetics for oxygen, as the one that best described growth of *Leptothrix discophora* SP-6 in the chemostat:

$$\mu = \mu_{\max} \frac{S_{\mathrm{p}}}{K_{\mathrm{sMp}} + S_{\mathrm{p}}} (1 - \mathrm{e}^{-S_{\mathrm{o}}/K_{\mathrm{sTo}}}) \qquad (11)$$

For the selected model, the biokinetic parameters are $\mu_{\max} = 0.576 \pm 0.021$ h^{-1}, $K_{\mathrm{sMp}} = 38.81 \pm 4.24$ mg L^{-1}, and $K_{\mathrm{sTo}} = 0.390 \pm 0.040$ mg L^{-1}. Figure 1 shows the specific growth rates predicted from eq 11 against those experimentally measured. The high correlation coefficient ($R^2 = 0.97$) demonstrates that the selected growth model accurately represents the growth of *Leptothrix discophora* SP-6.

Table 4. Growth Models, Biokinetic Parameters, and SSD[a]

multiple model eq no.	model no.	single model eq no. for pyruvate	single model eq no. for oxygen	μ_{max} (h^{-1})	K(p) (mg L^{-1})	K(o) (mg L^{-1})	λ_P	λ_O	B_P[b]	B_O[c]	SSD
1	8	4	5	0.5763	38.9829	0.3944					0.0054
1	13	5	5	0.5007	40.6310	0.4269					0.0056
1	23	7	5	0.5622		0.4106			0.2995		0.0058
1	12	5	4	0.5321	38.0799	0.2967					0.0110
1	15	5	7	0.5316	37.4906					0.0027	0.0121
1	7	4	4	0.6057	36.2021	0.2731					0.0142
1	22	7	4	0.5929		0.2874			0.2781		0.0145
1	10	4	7	0.6031	35.3772					0.0025	0.0152
1	25	7	7	0.5894					0.2739	0.0026	0.0172
1	17	6	4	0.5442	192.2085	0.3283	34.5957				0.0203
3	11	5		0.3742	34.4625						0.1404
3	6	4		0.4055	26.6233						0.1473
3	21	7		0.3964					0.2089		0.1509
1	14	5	6	0.4900	37.4601	67.4615		23.4690			0.3582
1	9	4	6	0.5587	35.8746	96.2865		24.5351			0.3585
1	24	7	6	0.5464		162.5678		214.3115	0.2862		0.3587
1	19	6	6	0.5418	43.3277	53.7801	1.0818	68.3582			0.3587
3	3		5	0.1738		0.1422					0.4526
1	18	6	5	0.1738	8.2754	0.1422	35.6069				0.4526
3	5		7	0.1735						0.0003	0.4592
1	20	6	7	0.1735	177.0147		128.8711			0.0003	0.4592
3	2		4	0.1728		0.0303					0.4596
3	1			0.1676							0.4622
3	16	6		0.1676	72.6072		47.9024				0.4622
3	4		6	0.1558		24.5984		42.5332			0.6948

[a] First column shows the type of the model used in the simulation (see eqs 1−3). The third and fourth columns show the equations we combined to assemble the double substrate kinetic expressions. The results are presented in ascending order of SSD. K(p), column 6, refers to K_{sMp}, K_{sTp}, K_{sMZp}, and K(o), column 7, refers to K_{sMo}, K_{sTo}, K_{sMZo}. [b] mg pyruvate mg^{-1} microorganism. [c] mg oxygen mg^{-1} microorganism.

Table 5. Models That Give the Best SSD[a]

	μ_{max} (h^{-1})	K_{sMp} (mg L^{-1})	K_{sTp} (mg L^{-1})	K_{sTo} (mg L^{-1})	B_P[b]	SSD
		Model no. 8				
		Pyruvate: 4 Oxygen: 5				
parameters from original data	0.5763	38.9829		0.3944		0.0054
av from simulated data	0.5758	38.8105		0.3903		0.0183
SD from simulated data	0.0212	4.4241		0.0390		0.0061
		Model no. 13				
		Pyruvate: 5 Oxygen: 5				
parameters from original data	0.5007		40.6310	0.4269		0.0056
av from simulated data	0.4988		40.7680	0.4189		0.0194
SD from simulated data	0.0072		3.9905	0.0424		0.0063
		Model no. 23				
		Pyruvate: 7 Oxygen: 5				
parameters from original data	0.5622			0.4106	1.2201	0.0058
av from simulated data	0.4796			0.3389	1.1303	0.1320
SD from simulated data	0.0790			0.0996	0.5624	0.0600

[a] The biokinetic parameters were calculated for experimental data and for simulated data sets. [b] mg pyruvate mg^{-1} microorganism.

Although our analysis shows that model 8 has the lowest SSD value, model 13 is not poor and can also be used to describe the growth of *Leptothrix discophora* SP-6. Model 23 has a very high average SSD value and was rejected, while models 12, 15, 7, 22, 10, 25, and 17 all have high SSDs and do not predict the specific growth rates (= dilution rate) in Table 3 as well as models 8 or 13.

Tessier's Growth Model and Monod Half Rate Constant. The coefficient K_{sT} in the Tessier equation should not be confused with the half rate coefficient K_{sM} in the Monod equation. Tessier (1942) developed his equation hypothesizing that the dependence of specific growth rate on the substrate concentration was proportional to the difference between μ and μ_{max}:

$$\frac{d\mu}{dS_i} = \frac{1}{K_{sT}}(\mu_{max} - \mu) \qquad (12)$$

Equation 12, when integrated, gives the well-known form of the Tessier equation (eq 5). To compare the Tessier coefficient K_{sT} with the Monod half rate coefficient K_{sM}, the half rate constant (substrate concentration for which $\mu = \mu_{max}/2$) can be estimated from eq 12 and is equal to K_{sT} log 2 (Powell 1974). In our model $K_{sTo} = 0.390$ mg L^{-1} corresponds to the half rate constant for oxygen in the Monod equation equal to $K_{sMo} = 0.39 \times \log 2 = 0.237$ mg L^{-1}.

Maintenance Coefficients and Yield Factors. The maintenance and yield factors for pyruvate and oxygen were calculated from Figures 2 and 3 and eqs 9b and 9c: $Y_{X/p} = 0.150$ mg microorganism (mg pyruvate)$^{-1}$, $Y_{X/o} = 1.24$ mg microorganism/mg oxygen, $m_p = 0.129$ mg pyruvate consumed (mg microorganism)$^{-1}$ h^{-1}, and $m_o = 0.076$ mg oxygen consumed (mg microorganism)$^{-1}$ h^{-1}.

The results of our measurements are in agreement with the results published by others. Emerson and

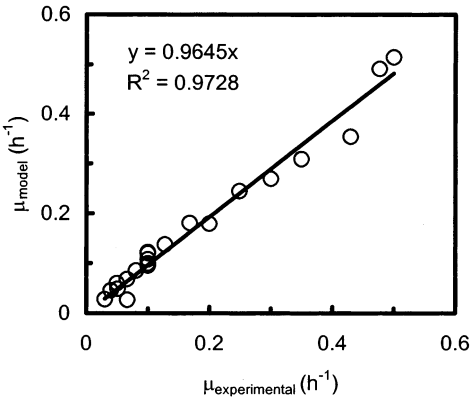

Figure 1. The specific growth rates, predicted from eq 11 versus experimentally measured.

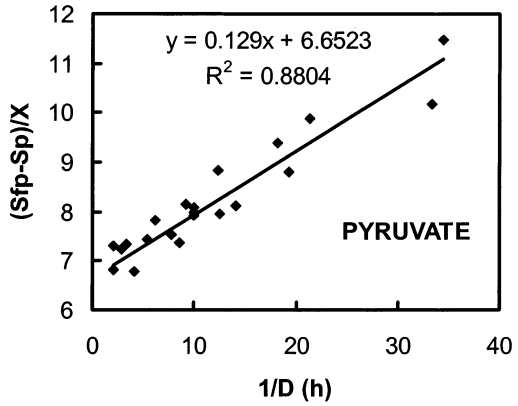

Figure 2. $(S_{fp} - S_p)/X$ versus $1/D$ for pyruvate. The slope of the line gives m_p and the intercept gives $1/Y_{X/p}$.

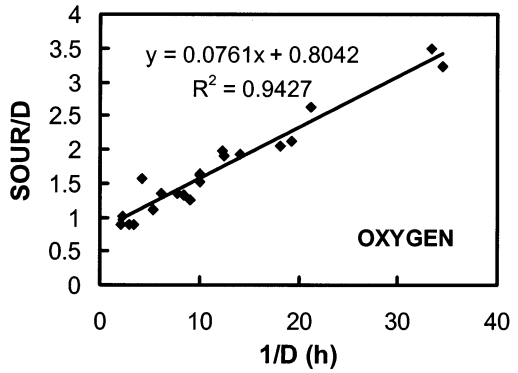

Figure 3. SOUR/D versus $1/D$. The slope of the line gives m_o and the intercept gives $1/Y_{X/o}$.

Ghiorse (1992) grew *Leptothrix discophora* SP-6 in MSVP and in PYG (peptone, yeast extract, glucose) media shaken at 150 rpm at 25 °C. They reported a maximum specific growth rate of 0.5 h^{-1} in both media, which is close to the maximum specific growth rate, 0.576 h^{-1}, estimated using our procedure. We could not find the yield coefficients for *Leptothrix discophora* SP-6 in the literature. However, the measured yield coefficients for pyruvate ($Y_{X/p} = 0.150$) and oxygen ($Y_{X/o} = 1.24$) are in the limits reported in the literature for other microorganisms grown on different carbon sources between 0.18 and 1.01 g g^{-1} and between 0.17 and 1.5 g/g for oxygen (Bailey and Ollis, 1986; Shuler and Kargi,1992).

Conclusions

(1) A double-substrate model, using Monod growth kinetics for pyruvate and Tessier growth kinetics for oxygen, has a high correlation with the chemostat data. Using this kinetic model, we calculated the following growth parameters for *Leptothrix discophora* SP-6: $\mu_{max} = 0.576 \pm 0.021$ h^{-1}, $K_{sMp} = 38.81 \pm 4.24$ mg L^{-1}, $K_{sTo} = 0.390 \pm 0.040$ mg L^{-1}, $Y_{X/p} = 0.150$ (mg microorganism/mg pyruvate), $Y_{X/o} = 1.24$ (mg microorganism (mg oxygen)$^{-1}$), $m_p = 0.129$ mg pyruvate consumed (mg microorganism)$^{-1}$ h^{-1}, and $m_o = 0.076$ mg oxygen consumed (mg microorganism)$^{-1}$ h^{-1}.

(2) We have developed an algorithm to estimate biokinetic parameters. This algorithm can be modified and used to predict biokinetic parameters from a variety of microbial species grown in chemostats. We hope that making this algorithm available may stimulate more frequent use of multiple microbial growth kinetics to describe the growth of different microorganisms.

Acknowledgment

The research was supported by the United States Office of Naval Research contract number N00014-99-1-0701 and by the cooperative agreement EED-8907039 between the National Science Foundation and Montana State University. The authors would like to thank Dr. Haluk Beyenal for his help with the mathematical modeling and experimental design, John Neuman for his help with HPLC analysis, and Dr. Phil Stewart for his comments and discussions.

Notation

B_i	constant in Contois model for substrate i (mg substrate/mg microorganism)
D	dilution rate (h^{-1})
K_{sMi}	Monod half saturation constant for substrate i (mg L^{-1})
K_{sTi}	Tessier saturation constant for substrate i (mg L^{-1})
K_{sMZi}	Moser constant for substrate i (mg L^{-1})
m_i	maintenance factor for limiting substrate i (mg microorganism (mg substrate i)$^{-1}$)
N	number of experiments (integer)
Q	volumetric flow rate (L h^{-1})
S_{ei}	substrate concentration in effluent stream (mg L^{-1})
S_{fi}	concentration of substrate i in influent stream (mg L^{-1})
S_i	concentration of substrate i (mg L^{-1})
SOUR	specific oxygen uptake rate (mg oxygen (mg microorganism)$^{-1}$ h^{-1})
SSD	sum of squares of difference
V	reactor volume (L)
X	microorganism concentration in chemostat (mg L^{-1})
$Y_{X/i}$	yield coefficient for limiting substrate i (mg microorganism (mg limiting substrate)$^{-1}$)

Greek letters

λ_i	Moser coefficient for substrate i
μ	specific microbial growth rate (h^{-1})
μ_i	specific microbial growth rate for the limiting substrate i (h^{-1})
μ_{max}	maximum microbial specific growth rate (h^{-1})
μ_{exptl}	experimentally determined microbial specific growth rate ($\mu = Q/V$) (h^{-1}).
μ_{model}	specific microbial growth rate predicted from the models (h^{-1})

Subscripts

i	substrate
n	NH_4^+
p	pyruvate
o	oxygen

Appendix A

The MATLAB code is presented in Charts 1 and 2 and consists of two files. The MATLAB *script file* is used to test all of the models presented in Table 1 and to calculate biokinetic parameters for these models. To calculate biokinetic parameters for a model we used

Chart 1. MATLAB Script File

```
1.  %  Biokinetic parameter finder
2.  %  This is MATLAB script file to find biokinetic parameters
3.  %
4.  %  Double_engine is the function which
5.  %     calculate sum of loss squares (loss)
6.  %     returns loss value
7.  %

8.  % global parameters used by engine function
9.  global Dilution;       % dilution rate
10. global Microorganism;  % microorganism concentration
11. global Pyruvate;       % pyruvate concentration
12. global Oxygen;         % oxygen concentration
13. global model_p;        % models for pyruvate
14. global model_o;        % models for oxygen
15. global n_of_data;      % number of data points


16. % ***************************************************************
17. % read experimental data
18. % to run using different data just change the data here
19. % ***************************************************************

20. % dilution rate
21. Dilution=[0.029;0.052;0.071;0.081;0.129;0.163;0.24;0.48;0.118;0.1;0.08;0.1;0.1; 0.1; 0.047;
    0.055;0.03;0.11;0.188;0.5;0.3;0.35;0.43];

22. % microorganism concentration
23. Microorganism=[87;113;131;110;111;97;143;106;134;104;175;109;125;175;114;121;98;119;132;
    99;103;121;113];

24. % pyruvate concentration
25. Pyruvate=[2;3.6;5.2;26.9;12.8;40.7;28.9;225;10.4;7.7;10.2;470;8.1;10.4;3.4;4.5;1.9;8.1;17.5;325;3
    4.1;74;234];

26. % oxygen concentration
27. Oxygen=[5.7;5.6;3.8;0.2;1.3;0.4;2.2;6.8;2.1;3.3;0.9;0.1;5.1;6;7.6;7.7;7.8;7.7;5.5;6.8;1.6;0.9;0.65];

28. n_of_data=size(Dilution);  % calculate number of data points
29. % this data file will be located same directory where MATLAB runs
30. fid = fopen('dataout.txt','w');

31. for model_p=0: 4   % models for pyruvate
32. for model_o=0: 4   % models for oxygen
33. for iteration=1: 1  % number of runs for different initial guesses
34. for i=1:7   % maximum 7 parameters to calculate
            x(i)=rand(1)*100;   % generate random initial values
35. end    % for i
36. %  Run minumum search algorithms for biokinetic parameters
37. [xx,fval]=fminsearch(@double_engine,[x(1),x(2),x(3),x(4),x(5),x(6),x(7)])
38. %  xx calculated parameters matrix- returned from fminsearch
39. %  ignore any unused parameter values as an example if the model requires
40. %  use of X(1) and X(2) you will see X(3), X(4).... in output
41. %  however they will not be used anywhere
42. % print results to data file
43. fprintf(fid,'%6.5f \t',model_p, model_o, xx,fval);
44. fprintf(fid,'\n');  % new line
45. % to see which model is currently running at runtime
46. disp(model_p); disp(model_o);
47. xx     % see calculated parameter on screen
48. fval   % see loss
49. end    % iteration
50. end    % model_o
51. end    %for loop

52. fclose(fid) % close file
```

Chart 2. Function *double_engine*

```
1.  %  function double_engine
2.  %
3.  %  Copyright
4.  %  Center for Biofilm Engineering
5.  %  Biofilm Structure and Function Researh Group
6.  %  Montana State University
7.  %  Bozeman, MT, USA
8.  %
9.  %
10. %  calculates loss values for model and experimental data

11. function f=double_engine(xx)

12. % global data
13. global Dilution;       % Dilution rate
14. global Microorganism;  % Microorganism concentration
15. global Pyruvate;       % Pyruvate concentration
16. global Oxygen;         % Oxygen concentration
17. global model_p;        % specific growth rate for pyruvate
18. global model_o;        % specific growth rate for oxygen
19. global n_of_data;      % number of experimental point

20. % ---------------------------------------------------------------------------
21. %  the following values controlled by fminsearch
22. %  fminsearch automatically changes their values
23. %  and double_engine function returns loss value
24. %  so fminsearch finds minumum loss and corresponding biokinetic parameters

25. % passed by function
26. Mmax=xx(1);    % maximum specific growth rate
27. Kpyr=xx(2);    % Monod or Tessier coefficient for pyruvate
28. KO=xx(3);      % Monod or Tessier coefficient for oxygen
29. Lpyr=xx(4);    % Moser  coefficient for pyruvate
30. LO=xx(5);      % Moser  coefficient for oxygen
31. Bpyr=xx(6);    % Constant in Contois model for pyruvate
32. BO=xx(7);      % Constant in Contois model for oxygen
33. % ---------------------------------------------------------------------------
34. loss=0; % initialize it to zero

35. for i = 1:n_of_data

36. %  for pyruvate
37. if model_p==0  mu_p=1; end % nothing
38. if model_p==1  mu_p=Pyruvate(i)/(Pyruvate(i)+Kpyr); end  % Monod
39. if model_p==2  mu_p=1-exp(-Pyruvate(i)/Kpyr); end        % Tessier
40. if model_p==3  mu_p=(1+Kpyr*Pyruvate(i)^(-Lpyr))^(-1); end  % Moser
41. if model_p==4  mu_p=Pyruvate(i)/(Pyruvate(i)+Bpyr*Microorganism(i)); end  % Contois

42. %  for oxygen
43. if model_o==0  mu_o=1; end % nothing
44. if model_o==1  mu_o=Oxygen(i)/(Oxygen(i)+KO); end  % Monod
45. if model_o==2  mu_o=1-exp(-Oxygen(i)/KO); end        % Tessier
46. if model_o==3  mu_o=(1+KO*Oxygen(i)^(-LO))^(-1); end  % Moser
47. if model_o==4  mu_o=Oxygen(i)/(Oxygen(i)+BO*Microorganism(i)); end  % Contois

48. mu=Mmax*mu_p*mu_o;       % calculate overall specific growth rate
49. loss=loss+(Dilution(i)-mu)^2;  % calculate SSD

50. end % end of for loop

51. f=loss; % this is return value
52. return
```

MATLAB's random function generator to produce initial estimates (line 34). Also, we added a loop to run the program for different initial estimates (line 33). The optimum biokinetic parameters that give a minimum SSD (eq 10) are calculated using the *fminsearh* function (line 37) by selecting parameters (biokinetic coefficients) and sending them to the *double_engine* function. The *double_engine* function uses these parameters to calculate SSD (eq 10). Depending on the SSD values, the *fminsearh* procedure simulates biokinetic parameters until it finds the biokinetic parameters that give the minimum SSD (Lagarias et al., 1998). We found the default MATLAB values satisfactory to limit convergence of the predicted parameters. Although we have numbered lines to document the code, it is not necessary for the MATLAB programs.

References and Notes

American Type Culture Collection Catalogue Bacteria and Phages, 18th ed.; American Type Culture Collection: Rockville, MD 1992.

Bailey, J. E.; Ollis, D. F. *Biochemical Engineering Fundamentals*, 2nd ed.; McGraw-Hill: New York, 1986; pp 500−507.

Bandyopadhyay, B.; Humhrey, E.; Taguchi, N. Dynamic measurement of the volumetric oxygen transfer coefficient in fermentation systems. *Biotechnol. Bioeng.* **1967**, *9*, 533−544.

Beyenal, H.; Tanyolac, A. A combined growth model of *Zoogloea ramigera* including multisubstrate, pH, and agitation effects. *Enzyme Microb. Technol.* **1997**, *21*, 74−78.

Contois, D. E. Kinetics of bacterial growth: Relationship between population density and spesific growth rate of continuous culture. *J. Gen. Microbiol.* **1959**, *21*, 40.

Dickinson, W. H.; Caccavo, F., Jr; Lewandowski, Z. The ennoblement of stainless steel by manganic oxide biofouling. *Corros. Sci.* **1996**, *38*, 1407−1422.

Dickinson, W. H.; Lewandowski, Z. Manganese biofouling and the corrosion behavior of stainless steel. *Biofouling* **1996**, *10*, 79−93.

Emerson, D.; Ghiorse, W. C. Isolation, cultural maintenance, and taxonomy of a sheath-forming strain of *Leptothtrix discophora* and characterization of manganese-oxidizing activity associated with the sheath. *Appl. Environ. Microbiol.* **1992**, *58*, 4001−4010.

Lagarias, J. C.; Reeds, J. A.; Wright, M. H.; Wright, P. E. Convergence properties of the Nelder-Mead Simplex Method in Low Dimensions. *SIAM J. Optim.* **1998**, *9*, 112−147.

Machado, R. J.; Grady, C. P. L., Jr. Dual substrate removal by an axenic bacterial culture. *Biotechnol. Bioeng.* **1989**, *33*, 327−337.

Monod, J. The growth of bacterial cultures. *Annu. Rev. Microbiol.* **1949**, *3*, 371−394.

Moser, A. *The Dynamics of Bacterial Populations Maintained in the Chemostat*, Publication 614; The Carnegie Institution: Washington, DC, 1958.

Neelemen, R.; Joerink, M.; Beuvery, C.; Boxtel T. van. Dual-substrate utilization by *Bordetella pertussis*. *Appl. Microbiol. Biotechnol.* **2001**, *57*, 489−493.

Olesen, B. H.; Avci, R.; Lewandowski, Z. Manganese dioxide as a potential cathodic reactant in corrosion of stainless steels. *Corros. Sci.* **2000a**, *42*, 211−227.

Olesen, B. H.; Nielsen, P. H.; Lewandowski, Z. Effect of biomineralized manganese on the corrosion behavior of C1008 mild steel. *Corrosion* **2000b**, *56*, 80−89.

Panikov, N. S. *Microbial Growth Kinetics*; Chapman & Hall, Conwoll, UK, 1995.

Powell, E. O. The growth rate of microorganisms as a function of substrate concentration. In *Microbial Growth*; Dawson, P. S. S., Ed.; Dowden, Hutchinson & Ross, Inc.: Stroudsburg, PA, 1974; p 316.

Press: W. H.; Teukolsky, S. A.; Vetterling W. T.; Flannery, B. P. *Numerical Recipes in Fortran The Art of Scientific Computing*, 2nd ed.; Cambridge University Press: New York, 1992; pp 684−687.

Shuler, M. L.; Kargi, F. *Bioprocess Engineering Basic Concepts*; Prentice Hall, Inc.: Englewood Cliffs, NJ, 1992; p 171.

Standard Methods for the Examination of Water and Wastewater no. 2540E: Fixed and Volatile Solids Ignited at 550 °C, 19th ed.; Eaton, A. D., Clesceri, L. S., Greenberg, A. E., Eds.; American Public Health Assoc.: Washington, DC, 1995.

Tessier, G. Croissance des populations bacterie'nnes et quantite'd'aliment disponible *Rev. Sci. Paris* **1942**, *3208*, 209.

Zhang, J., Lion, L. W.; Nelson, Y. M.; Shuler, M. L.; Ghiorse, W. C. Kinetics of Mn(II) oxidation by *Leptothrix discophora* SS1. *Geochim. Cosmochim. Acta* **2002**, *65*, 773−781.

Accepted for publication June 5, 2002.

BP0255098